Solvent Effects on the Optical Properties of PEG-SH and CTAB Capped Gold Nanorods

M. Wielgus[a,*], M. Gordel[b], M. Samoć[b] and W. Bartkowiak[a]

[a]Department of Physical and Quantum Chemistry, Faculty of Chemistry, Wrocław University of Technology,
Wybrzeże Wyspiańskiego 27, 50-370 Wrocław, Poland
[b]Advanced Materials Engineering and Modelling Group, Faculty of Chemistry, Wrocław University of Technology,
Wybrzeże Wyspiańskiego 27, 50-370 Wrocław, Poland

Cetyltrimethylammonium bromide (CTAB) and (11-mercaptoundecyl)tetra(ethylene glycol) (PEG-SH) capped gold nanorods were prepared and dispersed in water and dimethyl sulfoxide (DMSO). Transmission electron microscopy images reveal that changing the solvent from water to DMSO cause that nanoparticles tend to organize (PEG-SH ligand) or aggregate (CTAB ligand). UV-vis absorbance spectra reveal that ligand as well as solvent exchange cause positive solvatochromic shifts and changes in the relative extinction values. After the transfer of nanorods from a solvent of lower to higher refraction index a red shift of the longitudinal surface plasmon resonance band is observed. This effect is more pronounced in the case of PEG-SH capped nanorods. Time resolved pump-probe measurements revealed that both ligand and solvent exchange influence the excited state relaxation times, however, a more pronounced change is induced by the ligand exchange. Two-photon excited fluorescence spectra of PEG-SH covered nanorods showed a slight intensity increase when moving from water to DMSO solvent.

1. Introduction

Influence of solvent on the UV-vis absorption spectra of organic molecules has been known for more than a century [1]. The term "solvatochromism" describes a modification of the position, intensity and sometimes the shape of the UV-vis absorption bands induced by the change in the polarity of the environment [1]. However, this definition has become broader recently, as it started to include new types of the environment such as ionic liquids [1–3], new areas of spectroscopy like fluorescence [4], two-photon absorption and two-photon fluorescence [5], and a broad range of materials including a variety of nanoparticles [6–20]. Nowadays, nanomaterials attract much attention from both fundamental scientists and engineers, due to their interesting properties and potential applications. Among the most promising nanoparticle varieties are the noble metal ones like e.g. gold nanorods (NRs), which are the focus of the present work. Their unique optical features are mainly due to the surface plasmon resonance (SPR) enhanced light scattering and absorption [21, 22]. While other shapes of plasmonic nanoparticles are also intensely studied, NRs have gained a significant interest due to their characteristic optical properties and have been investigated in the different contexts including both fundamental and application approaches [21–37]. They are promising as materials useful for areas such as biosensing [26, 30, 31], two-photon imaging [32, 33], gene and drug delivery [34, 35] and photothermal and photodynamic therapies [36, 37].

In this work we focus on the solvent effects on the optical properties of NRs. This approach was previously taken by Chen et al. [12] and Zhao et al. [13]. Chen et al. have prepared the NRs stabilized with CTAB and dispersed them in water–glycerol liquid mixtures of various volume ratios. They have reported a red shift of the longitudinal surface plasmon (l-SPR) peak with the increasing amount of glycerol [12]. Zhao et al. have prepared a colloidal solution of the NRs covered by PEG-SH and transferred them to different organic solvents. They have reported the quenching phenomena of two-photon photoluminescence when the NRs were dispersed in organic solvents compared to the water colloids. In their opinion the described effect was caused by electron transfer from electron-donating solvents to the excited NRs. Additionally, they performed transient absorption pump-probe measurements of the colloidal solution of the NRs in water and two organic solvents — diethylene glycol (DEG) and dimethylformamide (DMF). As a result, they have detected a different decay behaviour of the NRs in water and other solvents [13].

Although there have been pioneering works reporting the solvent effects on the NRs [12, 13], this highly interesting topic is still not sufficiently explored. In the present work we report on the solvent effects on optical properties of colloidal NRs covered by PEG-SH (PEG-SH@NRs) and CTAB (CTAB@NRs) dispersed in water and DMSO. On the basis of UV-vis and two-photon excited fluorescence (TPEF) spectra as well as ultrafast time-resolved pump-probe transmission measurements we present the analysis of the influence of the surfactant and solvent on the optical properties of the NRs.

*corresponding author; e-mail:
malgorzata.wielgus@pwr.edu.pl

2. Material and methods

Gold(III) chloride trihydrate ($HAuCl_4 \cdot 3H_2O$), sodium borohydride ($NaBH_4$), ascorbic acid, silver nitrate ($AgNO_3$), CTAB, PEG-SH, and DMSO were purchased at Sigma Aldrich and used as received. The NRs were synthesised according to the procedure introduced by Sau and Murphy [38]. First, a solution of the seed nanoparticles (spherical, 3.5 nm diameter) was prepared through the reduction of gold(III) chloride trihydrate by sodium borohydride (reduction of Au^{3+} to Au^0) and CTAB was used as a capping agent. This step was followed by the growth procedure, in which the gold salt was reduced by ascorbic acid in the presence of CTAB micelles. In order to obtain an appropriate aspect ratio of the NRs, a suitable concentration of silver nitrate was added to the reaction mixture. The reaction was performed for 1.5 h at 29 °C. As the next step, the growth solution was transferred into centrifuge tubes and centrifuged twice at 10 kRCF for 20 min. Finally, the solution of NRs capped by CTAB was resuspended in 10 mL of water. In order to exchange the CTAB ligand by PEG-SH, 200 μL of freshly prepared nanorods was mixed with 1 μL of 10 µM PEG-SH and left overnight on a shaker. The obtained solution was centrifuged twice at 6.4 kRCF for 15 min and then dispersed in water and DMSO. For comparison, a second batch of CTAB capped nanoparticles was prepared, which, after centrifugation, were directly dispersed in the selected solvents (without modification by the PEG-SH ligand).

3. Experimental

Transmission electron microscopy (TEM) images were taken by a high-resolution FEI Tecnai G^2 20 X-TWIN TEM microscope, equipped with LaB_6 electron gun cathode and CCD FEI Eagle 2K camera. The accelerating voltage was 200 kV. Images were taken for the CTAB and PEG-SH covered NRs. Samples were prepared in water and DMSO, 20 μL of each colloidal solution was placed on a separate TEM grid and left to dry. After solvents evaporated the samples were studied sequentially under the microscope in the same way. UV-vis extinction spectra were measured in 10 mm quartz cells (Hellma) using a Jasco V-670 spectrophotometer. Two-photon excited fluorescence spectra were recorded using a femtosecond Quantronix Integra-C regenerative amplifier. The laser generates $\approx$ 130 fs pulses at a repetition rate of 1 kHz. The excitation wavelength was 800 nm. The laser beam was attenuated using neutral density filters and directed onto the sample mounted in an Ocean Optics CUV-FL-DA Cuvette Holder. The emission signal was collected at the direction perpendicular to the excitation. A short-pass glass filter with a cutoff at $\approx$ 750 nm was put between the sample and the detecting system. The output emission signal was coupled into an optical fibre and sent to an Ocean Optics USB2000 + CCD spectrograph. The obtained data were transferred to a computer equipped with the Ocean Optics dedicated software. Ultrafast transient absorption pump-probe measurements were performed on the NRs suspensions in

1 mm glass cuvettes. For those measurements the 800 nm pulses from the Integra-C were fed into a Quantronix Palitra optical parametric amplifier (OPA) that converted them into 960 nm at a pulse width of $\approx$ 130 fs (the pulse width was measured in the same pump–probe measurement setup, by replacing the sample with a BBO crystal and analysing the autocorrelation signal). In order to obtain the pumping and probing beams, the output beam from the OPA was split into two. The pumping beam was directed to a motorized delay line and focused on the sample (lens focal length 50 mm), whereas the probe beam was attenuated by neutral density filters and also focused on the sample. Both beams were overlapped in the sample volume. Shortening of the pump beam optical path was leading to the increase of the probe-to-pump delay time giving a possibility to obtain time-resolved data. Changes of the pump beam power passing through the sample were detected by a photodiode connected to a lock-in amplifier (signal recovery). In order to synchronize the lock-in amplifier the pump beam was chopped at the frequency of 165 Hz. Determination of the excited states decay times was performed by theoretical calculations based on the convolution of the pump and probe pulses and taking into account variable delay times. The best fits of the theoretical decay curves to the experimental results have been achieved assuming a double-exponential decay model.

4. Results and discussion

The NRs investigated in this work were covered by two types of ligands: CTAB and PEG-SH. Both types of nanomaterial were transferred to water and DMSO. As it can be seen in Fig. 1c and d, the PEG-SH capped NRs are well dispersed in both solvents, however, in water the
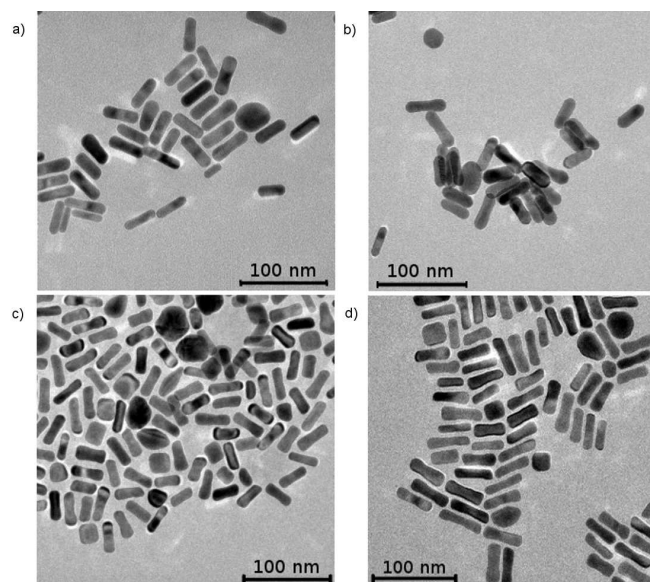

Fig. 1. The NRs covered by CTAB and PEG-SH in water and DMSO: (a) CTAB in water, (b) CTAB in DMSO, (c) PEG-SH in water, and (d) PEG-SH in DMSO.

NRs are distributed randomly, whereas in DMSO one can see some indications of self-organization. One can notice clusters, in which the NRs are arranged mutually parallel. In the case of the NRs covered by CTAB (Fig. 1a and b), in water the TEM images show that NRs are also dispersed. In the case of CTAB@NRs in DMSO one can see the tendency to create bigger groups composed of nanoparticles, which indicates a tendency of aggregation. It was reported before that the layer of CTAB can be destroyed by interaction with the organic solvent [13] which can be believed to be the main reason of aggregation process. Solutions of PEG-SH@NRs in water and DMSO as well as CTAB@NRs in water were clear and violet, while the solution of CTAB@NRs in DMSO was blue, yet still clear. All above, together with the absorption bands presented in Fig. 2, leads to the conclusion that only in the case of CTAB capped NRs in DMSO there exists a probability of nanoparticles aggregation.
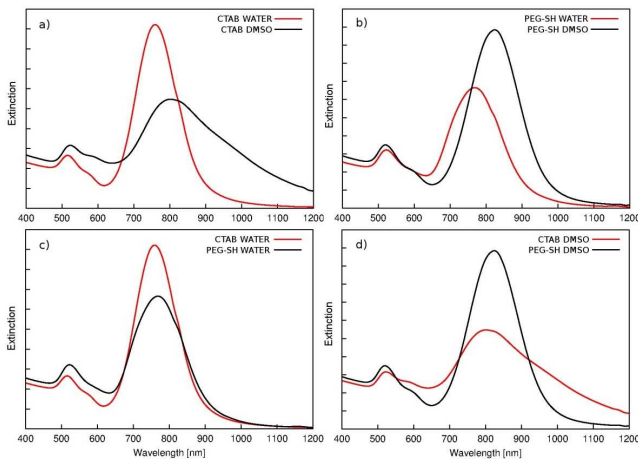

Fig. 2. UV-vis extinction spectra of: (a) CTAB capped NRs in water and DMSO, (b) PEG-SH capped NRs in water and DMSO, (c) CTAB and PEG-SH capped NRs in water, and (d) CTAB and PEG-SH capped NRs in DMSO.

Figure 2 presents the extinction spectra for four cases providing the comparison for the same ligand and two different solvents (Fig. 2a and b) and comparison for the same solvent, but different ligands (Fig. 2c and d). As it can be seen, in all cases the spectra maintain the features typical for the NRs, that is, there are two absorption bands (containing also scattering contributions) arising from transverse and longitudinal surface plasmon resonance. However, in the case of CTAB capped NRs in DMSO the l-SPR band is significantly suppressed and broadened compared to the CTAB@NRs in water, which can be an additional indication of an aggregation process. Both the ligand and solvent exchange cause l-SPR absorption band shifts (cf. Fig. 2 and Table I). Upon the solvent refraction index increase ($n_{\text{water}} = 1.3330$ [1]; $n_{\text{DMSO}} = 1.4793$ [1]), a significant red shift of the l-SPR band for both CTAB@NRs and PEG-SH@NRs, of 43 and 53 nm, respectively, is observed. This fact

is consistent with the previous reports that the l-SPR band is highly sensitive to the refractive index of the surrounding media [13, 39, 40]. Additionally, the red shift of l-SPR related to the ligand exchange was observed. The value of the red shift between CTAB@NRs and PEG-SH@NRs is approximately 10 nm in water and 19 nm in DMSO. This fact can be related to the slight differences in refractive indices of the investigated surfactants ($n_{\text{CTAB}} = 1.435$ [31], $n_{\text{PEG-SH}} = 1.475$ [41]), which causes decrease of the plasmon energy [42].

TABLE I

Summary of the spectroscopic data.

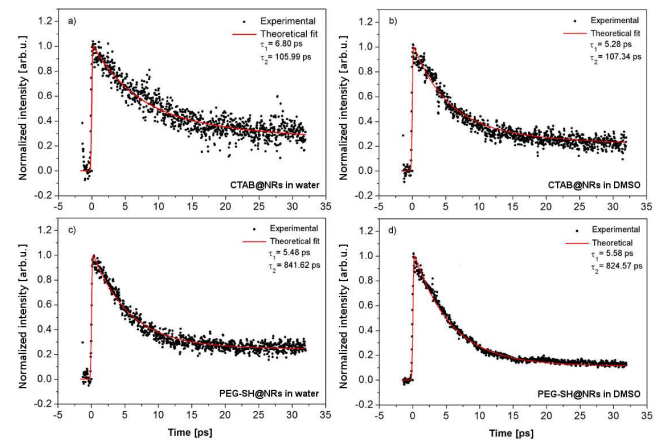| Ligand	Solvent	$\lambda_{\max}$ [nm]	$\Delta\lambda_{\max}$ [nm]	τ_1 [ps]	$|\Delta\tau_1|$ [ps]	τ_2 [ps]	$|\Delta\tau_2|$ [ps]
CTAB	water	758	43	6.80	1.52	105.99	1.32
	DMSO	801		5.28		107.31	
PEG-SH	water	768	52	5.48	0.10	841.62	17.05
	DMSO	820		5.58		824.57	

Fig. 3. Experimental data and theoretical fitting for relaxation dynamics of (a) CTAB capped NRs in water, (b) CTAB capped NRs in DMSO, (c) PEG-SH capped NRs in water, and (d) PEG-SH capped NRs in DMSO.

Time resolved pump–probe measurement data obtained for the investigated samples are presented in Fig. 3 and in Table I. This type of experiment enables observation of the optical response of the investigated material after excitation with ultrashort laser pulses. According to the literature, during the measurements the pump pulse excites the electrons and heats the electron gas to high temperatures. At the beginning of the process a non-Fermi electron distribution is created, reaching an internal thermal equilibrium through the electron–electron scattering (time scale ≈ 100 fs). Then the electron gas is cooled by electron–phonon interactions (time scale of a few ps) until the temperatures of the electron gas and lattice are equal. The last stage is the phonon–phonon (time scale of tens to hundreds of ps) interactions with the surrounding medium and complete relaxation of the absorbed energy [13, 22]. Due to the time scale of the

electron–electron scattering in our measurements, this process was not properly resolved, however the two other processes were registered.

Data were obtained using the same wavelength (960 nm) for pump and probe. The time constant describing the electron–phonon interactions (τ_1) was in the range of 5.28–6.80 ps. The highest value was observed in the case of CTAB@NRs in water, whereas the shortest one was registered for CTAB@NRs in DMSO. A more pronounced change was observed in the case of the second time constant (τ_2) when exchanging the ligands from CTAB to PEG-SH. The values changed from 105.99 ps and 107.31 ps obtained for CTAB@NRs in water and DMSO, respectively to 841.62 ps for PEG-SH@NRs in water and 824.57 ps in the case of PEG-SH@NRs in DMSO.

This situation is depicted in Fig. 3. Interestingly, no significant difference was observed between the nanorods in water and DMSO (for both CTAB and PEG-SH). This is in contrast with the data obtained by Zhao et al. [13]. They, indeed, have observed long time constants for PEG-SH capped NRs but only in the organic solvents (DMF and DEG), whereas in water such a long time constant was absent. They have explained the existence of the long time constants in the organic solvents, as a result of formation of charge-transfer complex between Au NRs and the DMF solvent possessing the lone pair of electrons. When the nanorods are photoexcited, the electrons are promoted to the *sp* band and form a hole in the *d* band. The created hole can be filled by electrons from the DMF solvent. In the pump–probe measurements they observed the temporal evolution of the charge separation and recombination processes [13]. However, no explanation was given why a similar process was absent in water. In our measurements we have observed the long time constant for PEG-SH@NRs both in water and DMSO. As both mentioned solvents have lone pairs of electrons, there is a possibility that we could have observed a similar process in both solvents. The long time constant was not detected in the case of CTAB@NRs both in water and DMSO, pointing out that processes described for PEG-SH@NRs are absent here. Concluding, our results indicate that the presence of the long time constant can be related to the ligand exchange rather than to solvent-induced processes.

We have also investigated the solvent effect on two-photon excited fluorescence of PEG-SH covered NRs on the basis of their TPEF spectra in water and DMSO. The obtained results are presented in Fig. 4a and c. In order to exclude the possibility of white light continuum generation effect in the solvent and cuvettes, we have compared the obtained results with those in pure solvents and limited the excitation intensity accordingly. The obtained emission spectra are broad, placed in the visible range and do not exhibit any fine structure, which is consistent with a previous report [13]. In this research we have observed an emission intensity increase when transferring the nanorods from water to DMSO. This increase

is also inconsistent with data reported by Zhao et al., who observed a two-photon photoluminescence quenching related to the previously described non-radiative recombination of electron–hole pairs [13]. As it was mentioned before, intensities of the observed emission are very low, therefore we can suppose that we have observed a similar quenching process in both solvents, however with slightly different efficiencies. In order to explain the details and confirm this possibility further research is required in the future.
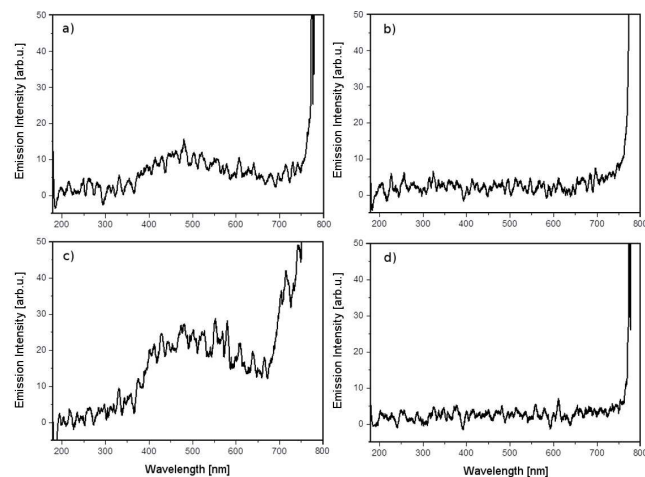

Fig. 4. Two-photon excited fluorescence spectra of PEG-SH capped NRs in (a) water and (c) DMSO. For comparison, spectra obtained for pure (b) water and (d) DMSO are provided..

5. Conclusions

In this work we have reported the preparation of CTAB and PEG-SH capped NRs dispersed in water and DMSO solvents. Except for CTAB@NRs in DMSO, the samples were well dispersed and showed no signs of aggregation. We have observed a red shift of the l-SPR band in the UV-vis absorption spectra with the increase of the solvent index of refraction. Moreover, we have observed red shift of the l-SPR when the ligand was exchanged from CTAB to PEG-SH, which was also assigned to the change of the refraction index of the surrounding medium. Time resolved pump-probe measurements were performed resulting in a conclusion that a change of surfactant from CTAB to PEG-SH prolongs the duration of the second time constant for the absorbance change decay, whereas changing the solvent did not cause any significant alteration in the relaxation processes. We suppose that, in the case of PEG-SH@NRs, we could have observed the effect of non-radiative recombination of electron–hole pairs in both investigated solvents described by Zhao et al. [13]. We have confirmed this discrepancy by performing the TPEF measurements for PEG-SH@NRs in water and DMSO and did not observe any significant differences between emission in water and DMSO. We suppose that also the fluorescence quenching could be present in both solvents.

References

[1] C. Reichardt, T. Welton, *Solvents and Solvent Effects in Organic Chemistry*, Wiley, Weinheim 2011.

[2] C. Reichardt, *Green Chem.* **7**, 339 (2005).

[3] C. Reichardt, *Chem. Rev.* **94**, 2319 (1994).

[4] J.R. Lakowicz, *Principles of Fluorescence Spectroscopy*, Springer Sci. and Business Media, New York 2007.

[5] M. Wielgus, W. Bartkowiak in: *Handbook of Solvents. Properties*, Vol. 1, Ed. G. Wypych, ChemTec Publishing, Toronto 2014, p. 695.

[6] C.A. Leatherdale, M.G. Bawendi, *Phys. Rev. B* **63**, 165315 (2001).

[7] S. Underwood, P. Mulvaney, *Langmuir* **10**, 3427 (1994).

[8] M. Lista, D.Z. Liu, P. Mulvaney, *Langmuir* **30**, 1932 (2014).

[9] S. Leekumjorn, S. Gullapalli, M.S. Wong, *J. Phys. Chem. B* **116**, 13063 (2012).

[10] Y. Li, X. Wang, S. Xu, W. Xu, *Phys. Chem. Chem. Phys.* **15**, 2665 (2013).

[11] I. Díez, M. Pusa, S. Kulmala, H. Jiang, A. Walther, A.S. Goldmann, A.H.E. Müller, O. Ikkala, R.H.A. Ras, *Angew. Chem. Int. Ed.* **48**, 2122 (2009).

[12] H. Chen, X. Kou, Z. Yang, W. Ni, J. Wang, *Langmuir* **24**, 5233 (2008).

[13] T. Zhao, X.-F. Jiang, N. Gao, S. Li, N. Zhou, R. Ma, Q.-H. Xu, *J. Phys. Chem. B* **117**, 15576 (2013).

[14] Y. Liao, X. Zhou, X. Xie, Q. Yu, *J. Mater. Sci. Mater. Electron.* **24**, 4427 (2013).

[15] M.K. Kavitha, P.C. Haripadmam, P. Gopinath, B. Krishnan, H. John, *Mater. Res. Bull.* **48**, 1967 (2013).

[16] M.Z. Rong, M.Q. Zhang, H.C. Liang, H.M. Zeng, *Appl. Surf. Sci.* **228**, 176 (2004).

[17] S.K. Ghosh, S. Nath, S. Kundu, K. Esumi, T. Pal, *J. Phys. Chem. B* **108**, 13963 (2004).

[18] K.L. Kelly, E. Coronado, L.L. Zhao, G.C. Schatz, *J. Phys. Chem. B* **107**, 668 (2003).

[19] S.A. Fischer, A.M. Crotty, S.V. Kilina, S.A. Ivanov, S. Tretiak, *Nanoscale* **4**, 904 (2012).

[20] S. Goel, K.A. Velizhanin, A. Piryatinski, S.A. Ivanov, S. Tretiak, *J. Phys. Chem. C* **116**, 3242 (2012).

[21] S. Eustis, M.A. El-Sayed, *Chem. Soc. Rev.* **35**, 209 (2006).

[22] S. Link, M.A. El-Sayed, *J. Phys. Chem. B* **103**, 8410 (1999).

[23] H. Chen, L. Shao, Q. Li, J. Wang, *Chem. Soc. Rev.* **42**, 2679 (2013).

[24] J. Olesiak-Banska, M. Gordel, R. Kolkowski, K. Matczyszyn, M. Samoc, *J. Phys. Chem. C* **116**, 13731 (2012).

[25] M. Gordel, J. Olesiak-Banska, K. Matczyszyn, C. Nogues, M. Buckle, M. Samoc, *Phys. Chem. Chem. Phys.* **16**, 71 (2013).

[26] J. Olesiak-Banska, M. Gordel, K. Matczyszyn, V. Shynkar, J. Zyss, M. Samoc, *Nanoscale* **5**, 10975 (2013).

[27] X. Wang, Z. Mei, Y. Wang, L. Tang, *Talanta* **136**, 1 (2015).

[28] L.T. Lanh, T.T. Hoa, N.D. Cuong, D.Q. Khieu, D.T. Quang, N. Van Duy, N.D. Hoa, N. Van Hieu, *J. Alloys Comp.* **635**, 265 (2015).

[29] X.-D. Wang, Z.-C. Luo, H. Liu, N. Zhao, M. Liu, Y.-F. Zhu, J.-P. Xue, A.-P. Luo, W.-C. Xu, *Opt. Commun.* **346**, 21 (2015).

[30] C.-Z. Li, K.B. Male, S. Hrapovic, J.H.T. Luong, *Chem. Commun.* **31**, 3924 (2005).

[31] C. Yu, J. Irudayaraj, *Anal. Chem.* **79**, 572 (2007).

[32] H. Wang, T.B. Huff, D.A. Zweifel, W. He, P.S. Low, A. Wei, J.-X. Cheng, *Proc. Natl. Acad. Sci. U.S.A.* **102**, 15752 (2005).

[33] N.J. Durr, T. Larson, D.K. Smith, B.A. Korgel, K. Sokolov, A. Ben-Yakar, *Nano Lett.* **7**, 941 (2007).

[34] C.-C. Chen, Y.-P. Lin, C.-W. Wang, H.-C. Tzeng, C.-H. Wu, Y.-C. Chen, C.-P. Chen, L.-C. Chen, Y.-C. Wu, *J. Am. Chem. Soc.* **128**, 3709 (2006).

[35] Q. Wei, J. Ji, J. Shen, *Macromol. Rapid Commun.* **29**, 645 (2008).

[36] T. Zhao, X. Shen, L. Li, Z. Guan, N. Gao, P. Yuan, S.Q. Yao, Q.-H. Xu, G.Q. Xu, *Nanoscale* **4**, 7712 (2012).

[37] X.H. Huang, I.H. El-Sayed, W. Qian, M.A. El-Sayed, *J. Am. Chem. Soc.* **128**, 2115 (2006).

[38] T.K. Sau, C.J. Murphy, *Langmuir* **20**, 6414 (2004).

[39] C. Wu, Q.-H. Xu, *Langmuir* **25**, 9441 (2009).

[40] L. Vigderman, B.P. Khanal, E.R. Zubarev, *Adv. Mater.* **24**, 4811 (2012).

[41] www.sigmaaldrich.com.

[42] E. Prodan, A. Lee, P. Nordlander, *Chem. Phys. Lett.* **360**, 325 (2002).